Int J Clin Exp Med 2017;10(11):15302-15308
www.ijcem.com /ISSN:1940-5901/IJCEM0047133

Original Article

High-intensity focused ultrasound ablation: an *in vitro* agarose gel model

Sen Yang[1,2,4*], Yi-Jing Chen[3*], Ran Cui[1], Hua-Xin Zhao[2], Yu Zhao[1], Zhu-Qing Liu[1], Yi Yu[1], Xiao-Yan Shao[1], Qing Xu[1,2]

[1]Department of Oncology, Shanghai Dermatology Hospital, Shanghai, China; [2]Department of Medical Oncology, Shanghai Tenth People's Hospital, School of Medicine, Tongji University, Shanghai, China; [3]Department of Pathology, Traditional Chinese Medicine Hospital of Kun Shan, Suzhou, Jiangsu, China; [4]Department of General Practice, Yangpu Hospital, Tongji University, Shanghai, China. [*]Equal contributors.

Received June 6, 2016; Accepted July 24, 2017; Epub November 15, 2017; Published November 30, 2017

Abstract: Purpose: There are many ultrasound studies involve the use of tissue-mimicking materials to research phenomena *in vitro* and predict *in vivo* biological effects. The goal of our study was to establish a typical agarose gel model of high-intensity focused ultrasound (HIFU) treatment for empirical study. Materials and methods: In this study, the model consists of human pancreatic tissues embedded in an agarose gel. The Sprague Dawley (SD) rat liver tissues were encapsulated in agarose gel and ablated by HIFU. The changes *in vitro* after ablation were assessed using ultrasonography, pathological examination, and histochemical staining. Results: After HIFU treatment, the results showed that the ultrasonic echo signal of the ablating region was strong, and the necrosis at the center of the ablation was monitored using hematoxylin and eosin (HE) staining. Shrinkage, chromatin condensation, nuclear condensation and fragmentation of the mouse liver cancer cells were assessed during pathological examination. Acid phosphatase (ACP) and succinic dehydrogenase staining (SDH) were negative in the experimental group. Discussion: Our study demonstrated that agarose model was appropriate for HIFU ablation in *in vitro* human tissues. The *in vitro* model may provide a useful tool for studying ablation induced by HIFU and facilitate further investigation of HIFU in anticancer therapeutics.

Keywords: High-intensity focused ultrasound, *in vitro* model, agarose gel, ablation

Introduction

HIFU induces coagulative necrosis of tumors without any skin damage, and is a truly noninvasive modality [1]. In addition to thermal ablation, changes in cellular and molecular responses occurred in the local environment of HIFU-ablated animal models [2].

Currently, *in vitro* animal model ablation is the most common modality for HIFU treatment. High-intensity focused ultrasound with pulmonary flooding generated a thermal effect *in vivo* in a porcine model of lung tumor [3]. Tumor-bearing mice were injected with micro-bubbles via tail vein and treated with HIFU to study the *in vivo* effect of HIFU on breast cancer cell lines [4]. A number of models have been used to simulate thermal lesion formation caused by ultrasound-induced heating in high-intensity focused ultrasound (HIFU) [5, 6]. While these can accurately mimic the response of soft tissues to heating, they are unable to precisely visualize or quantify mechanical ablation caused by HIFU compared with human tissues.

A human tissue model for measurement of HIFU treatment would be valuable in both ultrasound imaging and therapy. It could verify whether a given transducer and set of acoustic parameters are capable of causing therapeutic effect. However, the use of HIFU in *in vitro* human models is limited, because most of the patients who receive HIFU treatment are contraindicated for surgery, and tissue samples are not easily available for study. We, therefore, developed a novel agarose gel model to investigate HIFU treatment in human tumor tissue samples. In this study, an *in vitro* model of liver for HIUF ablation was established by encapsulating liver tissue in agarose gel.

Materials and methods

Tissue preparation

Eighteen SD rats aged between 6 and 8 weeks were purchased from the Shanghai Institutes for Biological Sciences, the Chinese Academy of Sciences, and raised in the central laboratory of Shanghai Tenth People's Hospital. After euthanasia, the rat liver tissues were divided randomly into three groups, six in each group, numbered 1, 2 and 3, respectively. Fresh human pancreatic cancer tissue was obtained from a department of pathology and placed in 0.9% saline solution at room temperature. All experiments were conducted within 6 hours of harvest. Experiments and animal care were carried out in compliance with the guidelines for the care and use of laboratory animals recommended by the Ministry of Science and Technology of the People's Republic of China [7].

HIFU

HIFU ablation was performed using a HIFU tumor therapy system (Model JC type, Chongqing Haifu Tech Co., Ltd, Chongqing City, China) comprising a firing system located in a degassed water tank, an imaging system consisting of an ultrasound scanner coupled with a sterotaxic localizing arm, and a computer-controlled system controlling the firing sequence and the three-dimensional movement of the firing head {Martin, 2014 #81; Marinova, 2016 #98} [8, 9].

Gel acoustics

Ultrasonic attenuation coefficient (UAC) is a parameter for acoustic propagation. The larger the value of UAC, the greater the sonic energy decrease [10, 11]. UAC was calculated using the insert-substitution method of GBT15261-2008 as follows (1) [12]:

$$\alpha = \frac{20}{d_1 - d_x} \log\left(A_s / A_1\right) + \alpha_w \quad (1)$$

Where α represents the UAC of tested material, and d_l is the thickness of the thicker sample, and d_x denotes the thickness of the thinner sample. A_s is the signal amplitude of thicker samples while A_1 is the signal amplitude of thinner samples. The α_W is the corrected value, and α and α_W are indicated as dB/cm. The units of d_1 and d_x are cm, and the A_s and A_1 are expressed in volts.

Preparation of in vitro agarose gel

Hydrogel was prepared by dissolving agarose (1% wt) in aqueous solvent at a temperature of 95°C. Gelation occurred when the temperature of this solution was lowered to room temperature. Briefly, rat liver tissues were encapsulated in 1% agarose. The agarose molds were allowed to gel at 37°C for 10 min and loaded into agarose scaffolds.

HIFU ablation

Eighteen SD rats were euthanized after fasting for 24 h. Liver tissues were obtained and evenly divided into three groups (blank, control, and experimental), and were loaded immediately on the scaffolds. The HIFU ablation was compliant with the guidance of the National Standard of China and described previously [13, 14]. The blank group of liver tissues was left untreated, while the control and experimental groups were encapsulated in agarose gel. The experimental group was ablated with the HIFU system (Model JC type, Chongqing HaifuTech Co., Ltd, Chongqing City, China) with a 10 cm diameter and 161 mm focal length was used as a therapy transducer. The transducer operates at 0.99 MHz, and is driven by a class D amplifier with matching network developed in our lab. The transducer was positioned in a tank of degassed, filtered water, and the focus was aligned to the cortex of the rats liver sample in plastic tubes filled with agarose gel submerged in the tank. A real-time ultrasound imaging device was used to locate the liver tissue as the predesigned target. Ultrasound was fired at a 3×3 grid of points sequentially, with 2 mm spacing between points. The total exposure time at each point was 5 seconds. The parameters used were 1.03 MHz, 400 W. This pattern was chosen over single spot treatments so that lesions were more easily located in tissue for histological sectioning. Eventually, the entire target region was covered by HIFU, leading to coagulation necrosis of the whole target region. During the therapeutic process, real-time evaluation of the profile of tissue damage in the model was conducted using the computer system and graphic analysis of the target field and the hyperecho of the tissues.

Table 1. Acoustic properties of PAA gel at various agarose powder concentrations

Agarose gel concentration	Sound speed (m/s)	acoustic attenuation (dB/cm)
0.5%	1503.88±1	0.04±0.01
1.0%	1503.19±1	0.07±0.02
2.0%	1503.31±1	0.11±0.01
4.0%	1510.05±1	0.20±0.01
8.0%	1526.50±1	0.46±0.02

Values are expressed as mean ± SD.

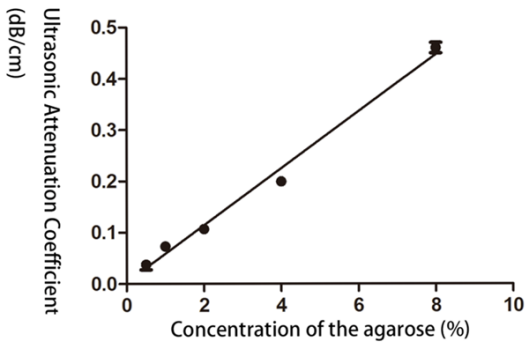

Figure 1. Gel acoustic characterization. Attenuation coefficient and agarose gel concentration. x coordinate representing agarose gel concentration (%), and y coordinate indicating the sound attenuation coefficient (dB/cm), with the trend line R2=0.990. The acoustic attenuation coefficient increased with increasing concentration of agarose gel.

Take a piece of human pancreatic cancer with a 4 cm diameter, then puts it into a plastic tube filled with agarose gel submerged in the tank. And then irradiated with HIFU, the process and parameters of HIFU ablation are the same as the rats liver tissue.

Hematoxylin and eosin (H&E) staining

The tissue samples were stained with 1% 2, 3, 5-triphenyltetrazolium chloride (TTC) solution for 5 to 7 min, and washed with water. Gross observations including the appearance, size and shape of the tissue were recorded. The tissue samples were fixed in 40 g/L formaldehyde solution, embedded in paraffin and stained with hematoxylin and eosin (H&E), respectively.

Histochemical staining

The liver samples were fixed in 40 g/L formaldehyde solution, embedded in paraffin and respectively stained with ACP and SDH, followed by light microscopy (Olympus BH2, Olympus Corporation, Tokyo, Japan). The samples were deemed positive if brown granules were detected in the cytoplasm following ACP staining, and if they stained blue purple with SDH.

Statistical analysis

Sound speed and acoustic attenuation were represented as mean ± S.D., and the significance level was set at $P<0.05$. The agarose concentration and acoustic attenuation were compared with linear analysis.

Results

Gel acoustics

The acoustic properties of our agarose gel at various agarose concentrations are summarized in this study (**Table 1**). The gel concentrations ranged from 0.5% to 8%. Gels with higher concentrations of agarose showed a higher acoustic attenuation (**Figure 1**). A significant correlation was found between the acoustic attenuation and agarose concentration, with a correlation coefficient of 0.990 ($P<0.01$). The magnitude of the attenuation coefficient was controlled easily between 0.03 and 0.5 (dB/cm), by varying the concentration of agarose.

In vitro agarose gel model and HIFU ablation

The agarose molds were allowed to gelate at 37°C for 10 min before loading on agarose scaffolds (**Figure 2A**). After HIFU treatment, changes in coagulation necrosis in the ultrasonic echo of the ultrasound model were clearly found in the center of the ablating region, and the intensity of the echo grew stronger after ablation (**Figure 2B**).

Pathological manifestations

After HIFU treatment, pale coagulation necrosis was easily identified in all the experimental liver samples. Normal liver tissues were red, whereas tissues of coagulation necrosis were white after TTC staining. In the experimental group, there was a sharp boundary between HIFU necrosis and viable tissue (**Figure 2C**).

Light microscopy

Under a light microscope, the following necrotic features were observed in the livers of experimental group: karyopycnosis and nuclear frag-

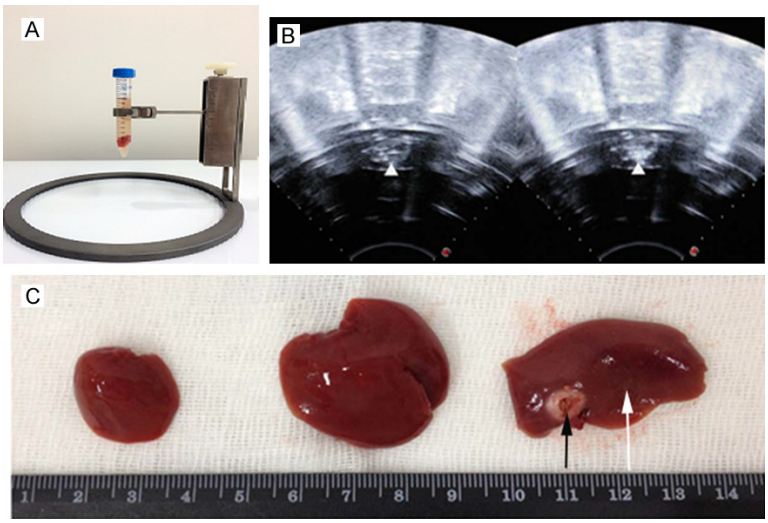

Figure 2. HIFU ablation. A. The in vitro model was loaded on agarose scaffolds. B. Changes in ultrasonic echo of the target regions after HIFU. [Δ]denotes the view of the coagulated lesion. C. These models were: blank, control and experimental groups (from left to right), respectively; TTC staining of liver tissues after HIFU. Coagulation necrosis (black arrow) was obvious and the white arrow showed normal pancreas. The boundary was clear.

mentation in most of the cells, and a sharp boundary between the normal tissue and target zones. The target tissues contained necrotic cells and nuclear debris after ablation and HE staining. Further, the experimental group stained negative with ACP and SDH. However, the control and blank groups showed no differences (**Figure 3A-I**).

Human pancreatic cancer tissue in HE staining

After HIFU treatment, the ablation area (A) showed homogeneous red dye and no cell structure, no ablation area (C) had clear cell structures and nucleolus, but the cells were arranged disorder. The junction between the two areas (B) could be seen the fuzzy structure, and nuclear pale staining (**Figure 4**).

Discussion

The ideal treatment for localized cancer should result in complete cell death without collateral damage [15, 16]. Previous researchers have directly observed the interaction of cavitation with cells, either with liquid and gel cell suspensions [17].

The novelty of our model as follows: we found that the tissue model described in this study can be used to directly observe cavitation and the resulting damage as it would occur in solid soft tissues [18]. Besides, the model provides a more controllable method to study the effects of different ultrasound parameters and transducers than *in vivo* tissue.

Agarose is a polysaccharide with alternating copolymers of 1,4-linked 3, 6-anhydro-α-l-galactose and 1,3-linked β-D-galactose. It has been commonly used as a gel for electrophoresis of nucleic acids in the laboratory [19, 20]. The agarose gel is stable and does not swell at constant temperature or re-liquefy until heated to 65°C [21]. Besides, it is easy to manufacture reproducibly. It is user-friendly, and amenable to large-scale use [22].

Acoustic attenuation coefficient demonstrated the ability of the media to transfer energy. A higher agarose gel concentration resulted in greater acoustic attenuation coefficient [23, 24]. Therefore, to reduce the acoustic attenuation of agarose gels, low concentrations of agarose gel are better than higher levels. However, if the agarose gel concentration is low, it is very soft and fragile, and the acoustic attenuation coefficient of 1% agarose gel is 0.073±0.001 dB/cm [25]. The human tissue sound attenuation coefficient is about 0.5 to 1.5 dB/cm/MHz [26]. It is far less than the human tissue attenuation coefficient and the ultrasonic attenuation is negligible. Furthermore, in preliminary experiments [27], a polypropylene model was used after HIFU treatment. Several bubbles were observed in the central rubber block, and the polypropylene plastic was destroyed, while 1% agarose gel model after HIFU treatment showed no reaction. These show similar appearance to HIFU treatment seen previously in agarose gels [28]. Therefore, 1% agarose gel was the optimal choice.

In this study, we selected the rat liver tissue as a sample. *In vitro* liver tissue wrapped with 1% agarose gel was exposed to HIFU. The patho-

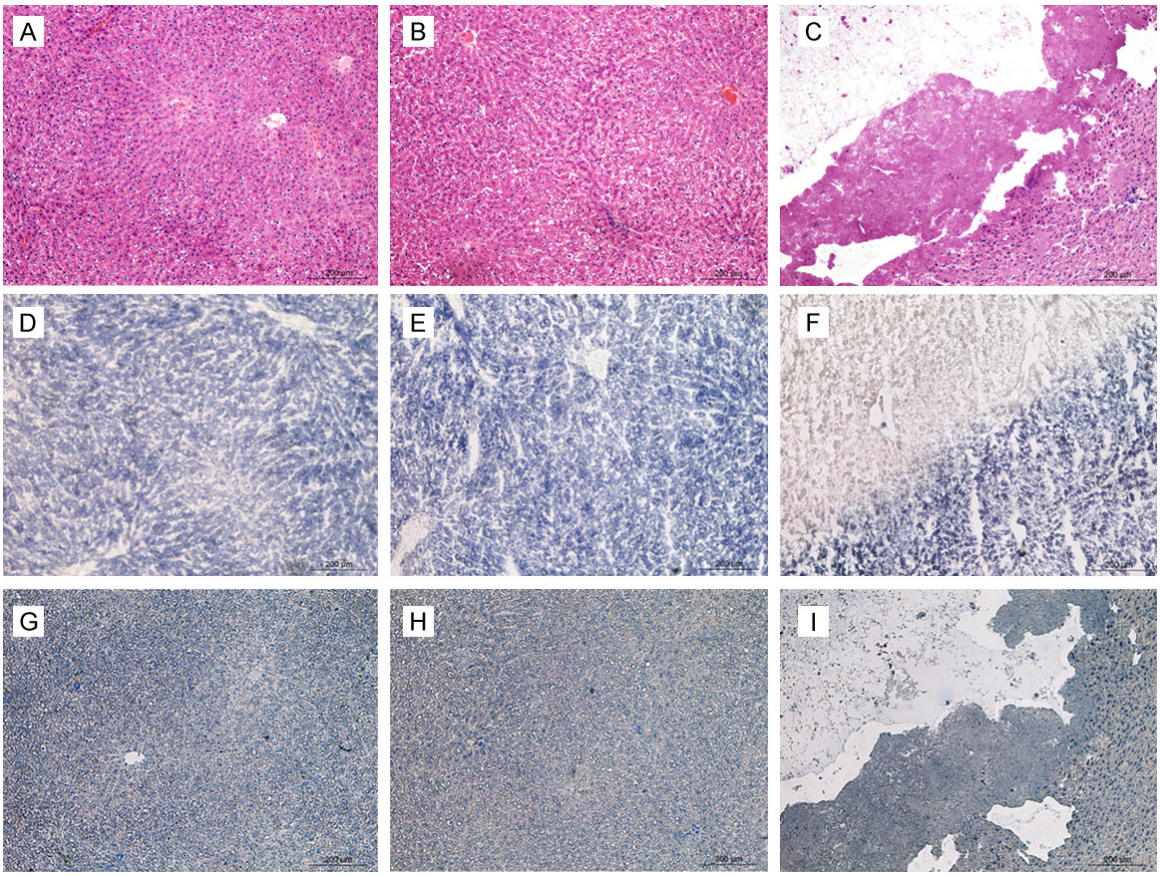

Figure 3. Light microscopy. Presentations of liver in the experimental group (C, F, I) under light microscope after HIFU (H&E, SDH, ACP×200). An apparent boundary was seen between normal and target tissues. However, no differences were found between the blank (A, D, G) and control groups (B, E, H). The cellular structures were normal.

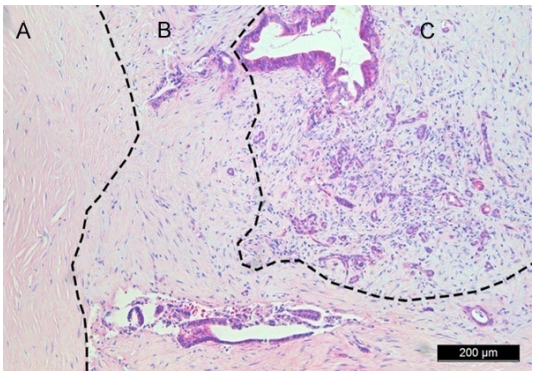

Figure 4. HE staining in human pancreatic cancer tissue. A: Coagulation necrosis area; B: The border area, cellular structure fuzzy, nuclear lightly stained; C: No ablated area, the cell structure was still visible and the nucleolus was clear, but the arrangement of cells were disordered (H&E×200).

logical section was observed under a microscope, which revealed that agarose gel had no effect on the biological properties of the tissue and HIFU ablation. Furthermore, we used human pancreatic cancer tissue to conduct experiments to confirm that this model was suitable for HIFU therapeutics, and this result was consistent with previous studies of *in vivo* tissue histotripsy lesions [29].

The model was simple and user-friendly facilitating tissue location and control. Each experiment in this model was treated with HIFU irradiation and ablative attenuation consistently, reducing the experimental error between the groups and any damage to the operator. Moreover, the gel model should be relatively simple and inexpensive to prepare, as one purpose is to avoid the costs associated with using experimental animals, and the experimental materials were wrapped in agrose gel, which prevented contamination of the tissue. Most importantly, this model was fixed by the bracket, obviating the need for manual handling.

However, additional trials are underway to ascertain the utility of agarose gel model. Besides, it is essential to determine the histological changes and molecular mechanisms of the agarose gel models. A number of preliminary studies suggested the reliability of the agarose model, which may facilitate additional studies investigating the mechanisms of carcinogenesis.

In conclusion, the novel agarose gel model is a safe and effective *in vitro* experimental tool for the investigation of HIFU anticancer therapeutics.

Acknowledgements

This article is supported by the National Natural Science Foundation of China (NO 81372749).

Disclosure of conflict of interest

None.

Address correspondence to: Dr. Qing Xu, Department of Medical Oncology, Shanghai Tenth People's Hospital, School of Medicine, Tongji University, 301 Middle Yanchang Road, Zhabei District, Shanghai 200072, P. R. China. Tel: +86 188 1787 9518; E-mail: qingxumd@aliyun.com

References

[1] Hsiao YH, Kuo SJ, Tsai HD, Chou MC and Yeh GP. Clinical application of high-intensity focused ultrasound in cancer therapy. J Cancer 2016; 7: 225-231.

[2] Kim YS, Bae DS, Park MJ, Viitala A, Keserci B, Rhim H and Lim HK. Techniques to expand patient selection for MRI-guided high-intensity focused ultrasound ablation of uterine fibroids. Am J Roentgenol 2014; 202: 443-451.

[3] Wolfram F, Reichenbach JR and Lesser TG. An ex vivo human lung model for ultrasound-guided high-intensity focused ultrasound therapy using lung flooding. Ultrasound Med Biol 2014; 40: 496-503.

[4] Wang J, Li P, Tian R, Hu W, Zhang Y, Yuan P, Tang Y, Jia Y and Zhang L. A novel microbubble capable of ultrasound-triggered release of drug-loaded nanoparticles. J Biomed Nanotechnol 2016; 12: 516-524.

[5] Kyriakou Z, Corral-Baques MI, Amat A, Coussios CC. HIFU-induced cavitation and heating in ex vivo porcine subcutaneous fat. Ultrasound 2011; 37: 568-579.

[6] Qian K, Li C, Ni Z, Tu J, Guo X and Zhang D. Uniform tissue lesion formation induced by high-intensity focused ultrasound along a spiral pathway. Ultrasonics 2017; 77: 38-46.

[7] Canney MS, Bailey MR, Crum LA, Khokhlova VA and Sapozhnikov OA. Acoustic characterization of high intensity focused ultrasound fields: a combined measurement and modeling approach. J Acoust Soc Am 2008; 124: 2406-2420.

[8] Merckel LG, Knuttel FM, Deckers R, Van DT, Schubert G, Peters NH, Weits T, van Diest PJ, Mali WP, Vaessen PH, van Gorp JM, Moonen CT, Bartels LW, van den Bosch MA. First clinical experience with a dedicated MRI-guided high-intensity focused ultrasound system for breast cancer ablation. Eur Radiol 2016; 26: 4037-4046.

[9] Möri N, Jud C, Salomir R and Cattin PC. Leveraging respiratory organ motion for non-invasive tumor treatment devices: a feasibility study. Phys Med Biol 2016; 61: 4247-4267.

[10] Martin JM, Handorf EA, Kutikov A, Uzzo RG, Bekelman JE, Horwitz EM and Smaldone MC. The rise and fall of prostate brachytherapy: use of brachytherapy for the treatment of localized prostate cancer in the national cancer data base. Cancer 2014; 120: 2114-2121.

[11] Hoche S, Hussein MA and Becker T. Density, ultrasound velocity, acoustic impedance, reflection and absorption coefficient determination of liquids via multiple reflection method. Ultrasonics 2015; 57: 65-71.

[12] Tang ZY, Zhao JN, Zhong WJ, Luo YD, Wu W, Chen WJ and Dai YB. The value of proton magnetic resonance spectroscopy in high-intensity focused ultrasound treatment of experimental liver cancer. Transl Oncol 2015; 8: 163-168.

[13] Poretti D, Lanza E, Sconfienza LM, Mauri G, Pedicini V, Balzarini L and Sardanelli F. Simultaneous bilateral magnetic resonance angiography to evaluate thoracic outlet syndrome. Radiol Med 2015; 120: 407-412.

[14] Li J, Krupka T, Yao J, Wang R, Jiang L, Zhou Y, Zuo G, Wang Z, Dai L and Ren J. Liquid-solid phase-inversion PLGA implant for the treatment of residual tumor tissue after HIFU ablation. PLoS One 2015; 10: e0117358.

[15] Zhou J, Zhou C, Zhan W, Jia X, Dong Y and Yang Z. Elastography ultrasound for breast lesions: fat-to-lesion strain ratio vs gland-to-lesion strain ratio. Eur Radiol 2014; 24: 3171-3177.

[16] Uchida T, Tomonaga T, Kim H, Nakano M, Shoji S, Nagata Y and Terachi T. Improved outcomes with advancements in high intensity focused ultrasound devices for the treatment of localized prostate cancer. J Urol 2015; 193: 103-110.

[17] Brunet T, Merlin A, Mascaro B, Zimny K, Leng J, Poncelet O, Aristégui C and Mondain-Monval O. Soft 3D acoustic metamaterial with negative index. Nat Mater 2015; 14: 384-388.

[18] Tako M, Kitajima S, Yogi T, Uechi K, Onaga M, Tamaki Y and Uechi S. Structure-function relationship of a gellan family of polysaccharide, S-198 gum, produced by alcaligenes ATCC31853. Advances in Biological Chemistry 2016; 6: 55-69.

[19] Maxwell AD, Cain CA, Duryea AP, Yuan L, Gurm HS and Xu Z. Noninvasive thrombolysis using pulsed ultrasound cavitation therapy-histotripsy. Ultrasound Med Biol 2009; 35: 1982-1994.

[20] Zucca P, Fernandez-Lafuente R and Sanjust E. Agarose and its derivatives as supports for enzyme immobilization. Molecules 2016; 21: 1577.

[21] Díazlópez A, Morenobueno G and Cano A. Role of microRNA in epithelial to mesenchymal transition and metastasis and clinical perspectives. Cancer Manag Res 2014; 2014: 205-216.

[22] Batumalay M, Harun SW, Ahmad F, Nor RM, Zulkepely NR and Ahmad H. Study of a fiber optic humidity sensor based on agarose gel. J Mod Optic 2014; 61: 244-248.

[23] Daugschies M, Rohde K and Barkmann R. The preliminary evaluation of a 1 MHz ultrasound probe for measuring the elastic anisotropy of human cortical bone. Ultrasonics 2014; 54: 4-10.

[24] Mohd TMK, Ibrahim S, Yunus MAM and Faramarzi M. Contact and non-contact ultrasonic measurement in the food industry: a review. Measurement Science & Technology 2016; 27: 012001.

[25] Feldmann A, Langlois C, Dewailly M, Martinez EF, Boulanger L, Kerdraon O and Faye N. Shear wave elastography (SWE): an analysis of breast lesion characterization in 83 breast lesions. Ultrasound Med Biol 2015; 41: 2594-2604.

[26] Martin NE, Massey L, Stowell C, Bangma C, Briganti A, Bill-Axelson A, Blute M, Catto J, Chen RC and D'Amico AV. Defining a standard set of patient-centered outcomes for men with localized prostate cancer. Eur Urol 2015; 67: 460-467.

[27] Zackrisson S, van de Ven SMWY and Gambhir SS. Light in and sound out: emerging translational strategies for photoacoustic imaging. Cancer Res 2014; 74: 979-1004.

[28] Misono S, Marmor S, Yueh B, Virnig BA. Treatment and survival in 10,429 patients with localized laryngeal cancer: a population-based analysis. Cancer 2014; 120: 1810-1817.

[29] Egorov V, Tsyuryupa S, Kanilo S, Kogit M and Sarvazyan A. Soft tissue elastometer. Med Eng Phys 2008; 30: 206-212.